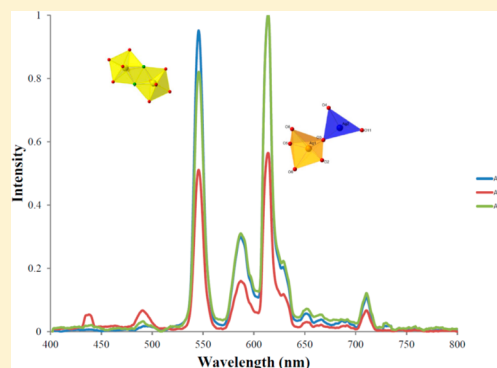


Three New Silver Uranyl Diphosphonates: Structures and Properties

Anna-Gay D. Nelson,^{*,†} Zsolt Rak,[‡] Thomas E. Albrecht-Schmitt,[§] Udo Becker,[†] and Rodney C. Ewing[†][†]Department of Earth & Environmental Sciences, University of Michigan, Ann Arbor, Michigan 48109-1005, United States[‡]Department of Materials Science & Engineering, North Carolina State University, Raleigh, North Carolina 27695, United States[§]Department of Chemistry and Biochemistry, Florida State University, Tallahassee, Florida 32306, United States

Supporting Information

ABSTRACT: The hydrothermal reaction of uranium trioxide and methylenediphosphonic acid in the presence of silver nitrate resulted in the formation of three new uranyl coordination polymers: $\text{AgUO}_2[\text{CH}_2(\text{PO}_3)(\text{PO}_3\text{H})]$ (**Ag-1**), $[\text{Ag}_2(\text{H}_2\text{O})_{1.5}]\{(\text{UO}_2)_2[\text{CH}_2(\text{PO}_3)_2]\text{F}_2\} \cdot (\text{H}_2\text{O})_{0.5}$ (**Ag-2**), and $\text{Ag}_2\text{UO}_2[\text{CH}_2(\text{PO}_3)_2]$ (**Ag-3**). All consist of uranyl pentagonal bipyramids that form two-dimensional layered structures. **Ag-1** and **Ag-3** possess the same structural building unit, but the structures are different; **Ag-3** is formed through edge-sharing of F atoms to form UO_5F_2 dimers. The pH and silver cation have significant effects on the structure that is synthesized. Raman spectra of single crystals of **Ag-1**, **Ag-2**, and **Ag-3** reveal ν_1 UO_2^{2+} symmetric stretches of 816 and 829, 822, and 802 cm^{-1} , respectively. Electronic structure calculations were performed using the projector augmented wave (PAW) method with density functional theory (DFT) to gain insight into the nature of bonding and electronic characteristics of the synthesized compounds. Herein, we report the syntheses, crystal structures, Raman spectroscopy, and luminescent behavior of these three compounds.



INTRODUCTION

During the past two decades, considerable research efforts have been focused on the rational design, synthesis, and understanding of metal phosphonates with different compositions and structures due to their potential applications in the fields of catalysis, ion exchange, magnetism, intercalation chemistry, and photochemistry.^{1–7} For *f*-element chemistry, their most important application is in separation processes due to the strong affinity of the phosphonate ($-\text{PO}_3$) group for the AnO_2^{2+} cation.^{8–10} Among the various mono- or diphosphonate ligands studied, methylenediphosphonate, and its derivatives, are unique due to the coordination geometries of metal ions.¹¹ Recently, we have synthesized a number of actinide diphosphonates, mainly with the methylenediphosphonate derivative in order to understand the relation of the structure to properties.^{12–16} These new compounds display a transition from the typical pillared-layered structure to one-dimensional chains, two-dimensional layers, and three-dimensional framework structures.^{17–20} In order to effectively prepare these new materials, a modification of the organic backbone of the phosphonate ligand is necessary. The addition of a carboxylate moiety results in homometallic^{21,22} and heterometallic compounds.^{23–28} Using phosphonic acids with amine and hydroxyl groups has resulted in a series of metal phosphonates with structures typical of simple phosphonates.^{29–31}

The architecture of actinide phosphonates can be further modified by the degree of protonation/deprotonation, as well as the presence of cations, anions, and neutral molecules in the reaction mixture that have an effect on the dimensionality of

the resulting structures.³² The use of organic structure-directors has been explored. Two-dimensional^{22,33} and pillared³⁴ structures form depending on the selection of the organic linker. Recently, a series of templated uranyl diphosphonates have been synthesized using methylenediphosphonate, which are all layered frameworks with extensive hydrogen-bonding, supramolecular networks.³⁵ Synthesis variables, such as the addition of “spectator” species, the incorporation of structure-directing agents, and charge-balancing counter-cations, influence product formation. As an expansion of the latter, three silver uranium diphosphonates are described and discussed in this paper: $\text{AgUO}_2[\text{CH}_2(\text{PO}_3)(\text{PO}_3\text{H})]$ (**Ag-1**), $[\text{Ag}_2(\text{H}_2\text{O})_{1.5}]\{(\text{UO}_2)_2[\text{CH}_2(\text{PO}_3)_2]\text{F}_2\} \cdot (\text{H}_2\text{O})_{0.5}$ (**Ag-2**), and $\text{Ag}_2\text{UO}_2[\text{CH}_2(\text{PO}_3)_2]$ (**Ag-3**). Electronic structure calculations and luminescent properties were also investigated in order to elucidate the effects of the silver center on structure formation.

EXPERIMENTAL TECHNIQUES

Syntheses. UO_3 (98%, International Bio-Analytical Industries), methylenediphosphonic acid, $\text{CH}_2(\text{PO}_3\text{H}_2)_2$ (98%, Alfa Aesar), silver nitrate $\text{Ag}(\text{NO}_3)$ (98%, Alfa Aesar), lithium hydroxide (98%, Alfa Aesar), and hydrofluoric acid (48 wt %, Alfa Aesar) were used as received. Reactions were run in PTFE-lined Parr 4749 autoclaves with a 23 mL volume. Distilled and Millipore filtered water was used in all reactions. Standard precautions were followed for handling radioactive materials when working with uranium. All reaction products were isolated by a thorough process of decanting the mother liquor to

Received: July 23, 2013

Published: February 13, 2014

obtain crystals. The crystals were then washed with distilled water, rinsed with methanol, and allowed to dry.

Ag₂UO₂[CH₂(PO₃)(PO₃H)] (Ag-1). UO₃ (287.5 mg, 1.005 mmol) was reacted with methylenediphosphonic acid (C1P2) (175.5 mg, 0.997 mmol), silver nitrate (176.4 mg, 1.038 mmol), and 3 mL of water. The reactants were loaded in a 23 mL Teflon Parr bomb. The reaction vessel was sealed and heated to 200 °C in a box furnace for 5 days. The autoclave was allowed to cool slowly to room temperature over a 24 h period by turning off the furnace. Pale yellow acicular prisms of Ag₂UO₂[CH₂(PO₃)(PO₃H)] were isolated. The approximate yield based on uranium content was 32%.

[Ag₂(H₂O)_{1.5}]{(UO₂)₂[CH₂(PO₃)₂F₂]}·(H₂O)_{0.5} (Ag-2). UO₃ (288.5 mg, 1.009 mmol) was reacted with methylenediphosphonic acid (C1P2) (176.0 mg, 1.00 mmol), silver nitrate (169.5 mg, 0.998 mmol), 0.2 mL of hydrofluoric acid, and 2 mL of water. The reactants were loaded into a 23 mL Teflon Parr bomb. The reaction vessel was sealed and heated to 200 °C in a box furnace for 5 days. The autoclave was allowed to cool slowly to room temperature over a 24 h period. Although the yield was low, yellow-red rectangular prisms of [Ag₂(H₂O)_{1.5}]{(UO₂)₂[CH₂(PO₃)₂F₂]}·(H₂O)_{0.5} were isolated. The approximate yield was 8% based on uranium content.

Ag₂UO₂[CH₂(PO₃)₂] (Ag-3). UO₃ (288.2 mg, 1.008 mmol) was reacted with methylenediphosphonic acid (C1P2) (176.0 mg, 1.000 mmol), silver nitrate (169.7 mg, 1.001 mmol), and 2 mL of 1 M LiOH. The reactants were loaded in a 23 mL Teflon Parr bomb. The reaction vessel was sealed and heated to 200 °C in a box furnace for 5 days. The autoclave was allowed to cool slowly to room temperature over a 24 h period. Yellow block shape crystals of Ag₂UO₂[CH₂(PO₃)₂] were isolated. The approximate yield based on uranium was 13%.

X-Ray Structure Refinements. Single crystals of Ag-1, Ag-2, and Ag-3 were isolated from their bulk reactions and mounted on a glass fiber. The intensity of the diffraction maxima was collected at -80 °C. The crystals were optically aligned on a Bruker APEXII Quazar X-ray diffractometer using a digital camera. Initial intensity measurements were performed using an IμS X-ray source, a 30 W microfocussed sealed tube (Mo Kα, λ = 0.71073 Å) with high brilliance and high-performance focusing Quazar multilayer optics. The intensities of diffraction maxima of a sphere were collected by a combination of four sets of exposures (frames). Each set had a different φ angle for the crystal, and each exposure covered a range of 0.3° in ω with an exposure time per frame of 10 to 30 s, depending on the crystal.

For all compounds, the determination of integrated intensities and global refinement were performed with the Bruker SAINT (v 6.02) software package using a narrow-frame integration algorithm. The data were treated with a semiempirical absorption correction by SADABS.³⁶ The program suite SHELXTL (v 6.12) was used for space group determination (XPREF), direct methods structure solution (XS), and least-squares refinement (XL).³⁷ The final refinements included anisotropic displacement parameters for all non-hydrogen atoms and a correction for secondary extinction when necessary. Key crystallographic details are given in Table 1. Atomic coordinates, bond distances, and additional structural information are provided in the Supporting Information (CIFs). Selected bond distances and angles can be found in Tables 2–5.

Powder X-Ray Diffraction (XRD). Powder X-ray diffraction patterns were collected for Ag-1, Ag-2, and Ag-3 on a Rigaku miniflex powder diffractometer equipped with a detector set for Cu Kα (λ = 1.5418 Å) radiation at room temperature in the angular range from 5° to 60° (2θ) with a scanning sampling width of 0.020° and scan speed of 1°/min. The observed and calculated patterns were compared to confirm that the single crystal was representative of the bulk, and both were in agreement. Powder XRD data are available as Supporting Information (Figures S1–S3).

UV–Vis–NIR and Fluorescence Spectroscopy. Fluorescence and absorption data were acquired from Ag-1, Ag-2, and Ag-3 compounds. The emission and absorption spectra were collected from single crystals using a Craic Technologies UV–visible–NIR Range Microspectrophotometer with a fluorescence attachment. The fluorescence spectra were recorded in the range of 400–800 nm at room temperature and achieved at an excitation wavelength of 365 nm

Table 1. Crystallographic Data and Structure Refinements for Ag₂UO₂[CH₂(PO₃)(PO₃H)] (Ag-1), [Ag₂(H₂O)_{1.5}]{(UO₂)₂[CH₂(PO₃)₂F₂]}·(H₂O)_{0.5} (Ag-2), and Ag₂UO₂[CH₂(PO₃)₂] (Ag-3)

compound	Ag-1	Ag-2	Ag-3
mass	549.87	997.77	657.74
color and habit	yellow, blocks	yellow, platelet	yellow, blocks
space group	<i>Pbca</i>	<i>C222₁</i>	<i>P2₁n</i>
<i>a</i> (Å)	12.0098(7)	9.2300(7)	7.9919(4)
<i>b</i> (Å)	10.3144(6)	13.2842(10)	12.5811(6)
<i>c</i> (Å)	12.2260(7)	11.1757(9)	8.1506(4)
<i>α</i> (deg)	90.00	90.00	90.00
<i>β</i> (deg)	90.00	90.00	96.2600(10)
<i>γ</i> (deg)	90.00	90.00	90.00
<i>V</i> (Å ³)	1514.48(15)	1370.29(18)	814.63(7)
<i>Z</i>	8	4	4
<i>T</i> (K)	193(2)	193(2)	193(2)
<i>λ</i> (Å)	0.71073	0.71073	0.71073
maximum 2θ (deg)	28.28	28.30	28.30
<i>ρ</i> _{calcd} (g cm ⁻³)	4.823	4.836	2.99
<i>μ</i> (Mo Kα)	24.379	26.694	24.999
<i>R</i> (<i>F</i>) for <i>F</i> _o ² > 2σ(<i>F</i> _o ²) ^a	0.0225	0.0226	0.0219
<i>R</i> _w (<i>F</i> _o ²) ^b	0.0773	0.0540	0.0527

^a*R*(*F*) = Σ||*F*_o - |*F*_c||/Σ|*F*_o|. ^b*R*_w(*F*_o²) = [Σ[*w*(*F*_o² - *F*_c²)²]/Σ*wF*_o⁴]^{1/2}.

Table 2. Selected Bond Distances (Å) and Angles (deg) for Ag₂UO₂[CH₂(PO₃)(PO₃H)] (Ag-1)

distance (Å)			
U(1)–O(8)	1.779(5)	P(1)–O(3)	1.521(5)
U(1)–O(7)	1.767(4)	P(1)–O(2)	1.523(6)
U(1)–O(2)	2.375(4)	P(1)–O(1)	1.542(4)
U(1)–O(1)	2.393(4)	P(1)–C(1)	1.812(6)
U(1)–O(6)	2.399(4)	P(2)–O(6)	1.517(4)
U(1)–O(4)	2.402(4)	P(2)–O(4)	1.524(5)
U(1)–O(3)	2.418(4)	P(2)–O(5)	1.556(4)
		P(2)–C(1)	1.799(7)
angles (deg)			
O(7)–U(1)–O(8)	173.8(2)		

Table 3. Selected Bond Distances (Å) and Angles (deg) for [Ag₂(H₂O)_{1.5}]{(UO₂)₂[CH₂(PO₃)₂F₂]}·(H₂O)_{0.5} (Ag-2)

distance (Å)			
U(1)–O(5)	1.781(5)	P(1)–O(1)	1.517(6)
U(1)–O(4)	1.787(6)	P(1)–O(3)	1.522(6)
U(1)–O(3)	2.319(5)	P(1)–O(2)	1.542(6)
U(1)–O(1)	2.324(5)	P(1)–C(1)	1.793(8)
U(1)–O(2)	2.373(5)	P'(1)–O'(2)	1.516(6)
U(1)–F(1)	2.344(5)	P'(1)–O'(1)	1.519(6)
U(1)–F(1)	2.334(5)	P'(1)–O'(3)	1.542(6)
		P'(1)–C(1)	1.805(8)
angles (deg)			
O(5)–U(1)–O(4)	178.7(3)		

from a mercury lamp. The absorption data were collected in a range of 200–800 nm at room temperature (see Supporting Information).

Raman Spectroscopy. Raman spectra were collected from single crystals of all compounds using a SPEX 1250 spectrometer with liquid nitrogen cooled CCD (Symphony) and a Verdis coherent laser (λ = 532.21 nm). A single crystal of each compound was placed on a glass slide from which the spectra were collected.

Table 4. Selected Bond Distances (Å) and Angles (deg) for Ag₂UO₂[CH₂(PO₃)₂] (Ag-3)

distance (Å)			
U(1)–O(8)	1.782(4)	P(1)–O(2)	1.523(3)
U(1)–O(7)	1.787(4)	P(1)–O(1)	1.531(4)
U(1)–O(2)	2.299(3)	P(1)–O(3)	1.538(3)
U(1)–O(6)	2.399(4)	P(1)–C(1)	1.799(5)
U(1)–O(4)	2.362(3)	P(2)–O(5)	1.514(4)
U(1)–O(3)	2.421(3)	P(2)–O(6)	1.525(4)
U(1)–O(1)	2.506(3)	P(2)–O(4)	1.539(4)
		P(2)–C(1)	1.803(5)
angles (deg)			
O(8)–U(1)–O(7)	177.26(16)		

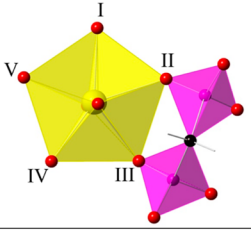
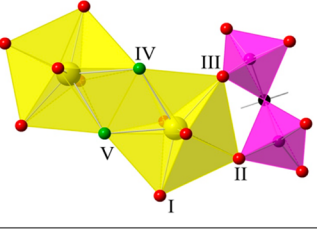
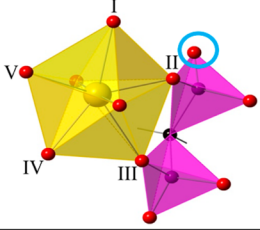
Electronic Structure Calculations. Electronic structure calculations have been performed using the projector augmented wave (PAW)^{38,39} method within density functional theory (DFT)^{40,41} as implemented in the Vienna Ab initio Simulation Package (VASP).^{42–45} The exchange-correlation potential was approximated by the generalized gradient approximation (GGA), as parametrized by Perdew, Burke, and Ernzerhof (PBE).⁴⁶ The standard PAW potentials, supplied with the VASP package, were employed in the calculations. The cutoff energy for the plane wave basis was set to 550 eV, and the convergence of self-consistent cycles was assumed when the energy difference between two consecutive cycles was less than 10^{−4} eV. As a result of convergence tests, all calculations were carried out using a 6 × 6 × 6 Monkhorst–Pack k-point mesh⁴⁷ and a Gaussian smearing of 0.1 eV. These values result in an accuracy of less than 1 meV/atom. The internal structural parameters were relaxed until the total energy and the Hellmann–Feynman forces on each nucleus were less than 0.02 eV/Å. In order to describe the behavior of the localized U 5f states, the orbital-dependent Coulomb potential (Hubbard *U*) and the exchange parameter *J* were included in the calculations within the DFT

+*U* method.^{48–50} The value of the Hubbard *U* parameter can be estimated from band-structure calculations in the supercell approximation with different *d* and *f* occupations.⁵¹ Here, we treat *U* and *J* as adjustable parameters using the following values: *U*(U_f) = 4.5 eV with *J*(U_f) = 0.5 eV. These values are physically reasonable and are within the range of values previously used in the literature.^{52–55}

RESULTS

Synthesis. Ag-1, Ag-2, and Ag-3 were prepared by the straightforward combination of the starting materials appropriate to each stoichiometry. Water, HF, and lithium hydroxide solution were used, respectively, in each reaction of Ag-1, Ag-2, and Ag-3. The purpose of this work was to study the influence of monovalent (silver) cations on structure formation in the uranium methylenediphosphonate system. Comparisons can be made among other diphosphonates in order to illustrate the diversity of structures in the uranium methylenediphosphonate system. Also, the addition of HF and LiOH solution affects the structures that form. In most cases, HF is generally added as a mineralizer to induce crystal nucleation and growth rather than as a constituent of the phase that forms. However, in Ag-2, fluoride incorporation was evident, as had been reported in previous work.^{28,56,57} The amount of HF must be carefully controlled in order to avoid isolation of uranium(IV) fluorides as the predominant product. The addition of LiOH raises the pH of the reaction and affects structure formation as seen in Ag-3. While the topologies of Ag-1 and Ag-3 are similar, it was observed that the addition of a small amount of hydroxide to the aqueous solution altered the topologies of the structure and the bonding environment. For Ag-2, the addition of HF to the reaction affects product formation, as dimers of (UO₅F)₂ pentagons are formed. Here, the addition of HF acts both as

Table 5. Summary of the Synthesized Compounds, Corresponding Solvent, and Structural Building Units (SBUs)^a

compound	space group	solvent	SBU	dimensionality
Ag-1	<i>Pbca</i>	H ₂ O		2-D
Ag-2	<i>C222</i> ₁	H ₂ O + HF		2-D
Ag-3	<i>P2</i> ₁ <i>n</i>	LiOH		2-D

^aThe blue circle in Ag-3 represents the phosphonate oxygen atom that solely binds to Ag⁺ centers.

a mineralizing agent and a ligand. In previous synthesized uranium methylenediphosphonate compounds that incorporated barium and organic amines, it was observed that the addition of a second metal center or template cation had an effect on the dimensionality and topologies that are formed in the uranium diphosphonate system. The powder diffraction patterns of the bulk products showed that the mixtures contained different phases, consisting of isolated silver uranium diphosphonate compounds and unreacted reagents, and perhaps some uranyl diphosphonates. The major products were the silver uranium diphosphonate compounds, which were identified as yellow acicular prisms, yellow-red rectangular prisms, and yellow blocked-shape crystals of **Ag-1**, **Ag-2**, and **Ag-3**, respectively, forming approximately 50% of the reaction products.

Structure of $\text{AgUO}_2[\text{CH}_2(\text{PO}_3)(\text{PO}_3\text{H})]$ (Ag-1**).** In **Ag-1**, each uranium center is located in a pentagonal bipyramidal coordination polyhedron, surrounded by seven oxygens, five of which are in the equatorial plane, and by three diphosphonate (C1P2) ligands. The remaining two oxygens are terminal and occupy the two axial positions, completing the coordination sphere of the U^{VI} center. The axial $\text{U}=\text{O}$ bond lengths vary from 1.767(4) to 1.799(5) Å, and equatorial $\text{U}-\text{O}$ bonds range from 2.375(4) to 2.418(4) Å. These distances result in a bond-valence sum of 5.98, which is consistent with U^{VI} .^{58,59} **Ag-1** consists of chelating and bridging PO_3 moieties of a single C1P2 ligand and uranyl ions, which form an anionic two-dimensional layer in the $[ac]$ plane (Figure 1a). The PO_3 groups of C1P2 chelate two uranium atoms, while also bridging to a third uranium. The remaining $\text{P}-\text{O}$ bond corresponds to a terminal oxygen atom and is therefore a protonated site with a distance of 1.556(4) Å. The uranyl units in this structure are connected by chelating PO_3 moieties of the C1P2 ligand, forming chains, which are cross-linked by a bridging PO_3 moiety of the same diphosphonate ligand creating a two-dimensional anionic sheet structure (Figure 1a). The Ag^+ ions reside between the layers and stitch the uranyl and phosphonate groups together (Figure 1b) so that the overall charged balance is maintained. The Ag^+ center is four-coordinated by four phosphonate oxygen atoms with distances ranging from 2.455(4) to 2.560(5) Å. Selected bond distances are compiled in Table 2.

Structure of $[\text{Ag}_2(\text{H}_2\text{O})_{1.5}]\{(\text{UO}_2)_2[\text{CH}_2(\text{PO}_3)_2\text{F}_2] \cdot (\text{H}_2\text{O})_{0.5}$ (Ag-2**).** Orthorhombic **Ag-2** ($C222_1$) consists of a single crystallographically unique U^{VI} metal center, one C1P2 ligand, and a single silver metal cation. The U^{VI} center forms edge-sharing dimers with F atoms and extends along the a axis. These dimers are chelated through PO_3 groups along the a axis and are further cross-linked by bridging PO_3 moieties to form two-dimensional anionic $\text{U}-\text{P}$ sheets parallel to the ac plane (Figure 2a). Each U^{VI} center is in the pentagonal bipyramidal geometry, coordinated by five oxygens, three of which are in the equatorial plane and are from two C1P2 ligands. The remaining two oxygens form the UO_2^{2+} cation and are terminal. The pentagonal geometry around the U^{VI} center is completed by two F ions in the equatorial plane. One C1P2 ligand binds four $(\text{UO}_3\text{F})_2$ dimers: two through chelation along the a axis and two through bridging PO_3 units down c . The $\text{U}-\text{P}$ sheets are held together by Ag^+ cations and molecular water that are located in the interlayer space, forming a corrugated, layered structure (Figure 2b,c).

The U^{VI} center is characteristically bound to two axial oxygen atoms to form the uranyl, UO_2^{2+} unit, with an average $\text{U}=\text{O}$

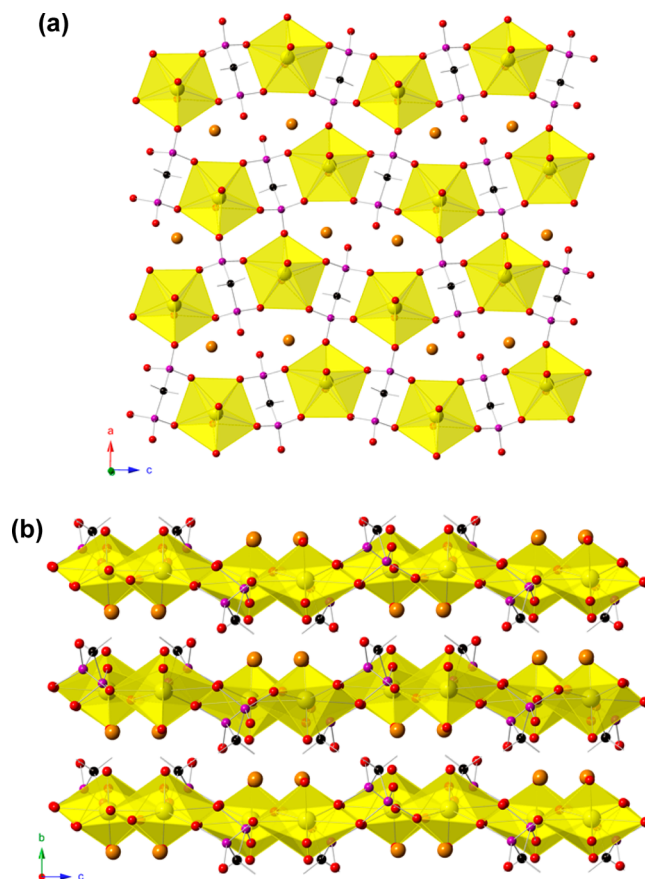


Figure 1. (a) Illustration of the sheets in $\text{AgUO}_2[\text{CH}_2(\text{PO}_3)(\text{PO}_3\text{H})]$ viewed along the ac plane. (b) Polyhedral representation of the uranyl phosphonate layers in $\text{AgUO}_2[\text{CH}_2(\text{PO}_3)(\text{PO}_3\text{H})]$; Ag^+ cations are located between the layers. The structure is constructed from UO_7 pentagonal bipyramids = yellow, silver = dark orange, oxygen = red, phosphorus = magenta, and carbon = black.

bond distance of 1.784(6) Å. Two F ions with bond lengths of 2.334(5) and 2.344(5) Å and an additional three oxygen atoms from the phosphonate ligand are bound to the uranyl cation in the equatorial plane with $\text{U}-\text{O}$ bond distances ranging from 2.318(4) to 2.373(5) Å. The assignments of F or O atoms are based on the improvement in the refinements when the correct element was selected. Energy dispersive X-ray spectroscopy (EDS) was used to also confirm the presence of F. Using the $\text{U}-\text{O}$ and $\text{U}-\text{F}$ distances a bond-valence sum of 5.80 for $\text{U}(1)$ is achieved, which is consistent with U^{VI} .^{58,59} The $\text{Ag}(1)$ cations are coordinated to both uranyl oxo atoms through apical positions and the basal plane to one phosphonate oxygen and two water molecules to form a trigonal bipyramidal geometry. The $\text{Ag}-\text{O}$ bond distances range from 2.279(4) to 2.589(5) Å. Selected bond distances are compiled in Table 3.

Structure of $\text{Ag}_2\text{UO}_2[\text{CH}_2(\text{PO}_3)_2]$ (Ag-3**).** **Ag-3** consists of a crystallographically unique uranyl group in the form of a pentagonal bipyramidal, one diphosphonate ligand, and two independent silver cations. The uranyl cations are linked through the phosphonate group by chelation into uranyl-phosphonate ($\text{U}-\text{P}$) chains along the a axis as shown in Figure 3a. These chains are further bridged by one of the remaining PO_3 groups to form $\text{U}-\text{P}$ sheets long ab plane (Figure 3a). The remaining phosphonate oxygen bonds to $\text{Ag}(1)$ and $\text{Ag}(2)$ by corner-sharing to form dimers (Figure 3b). The layers of $\text{U}-\text{P}$

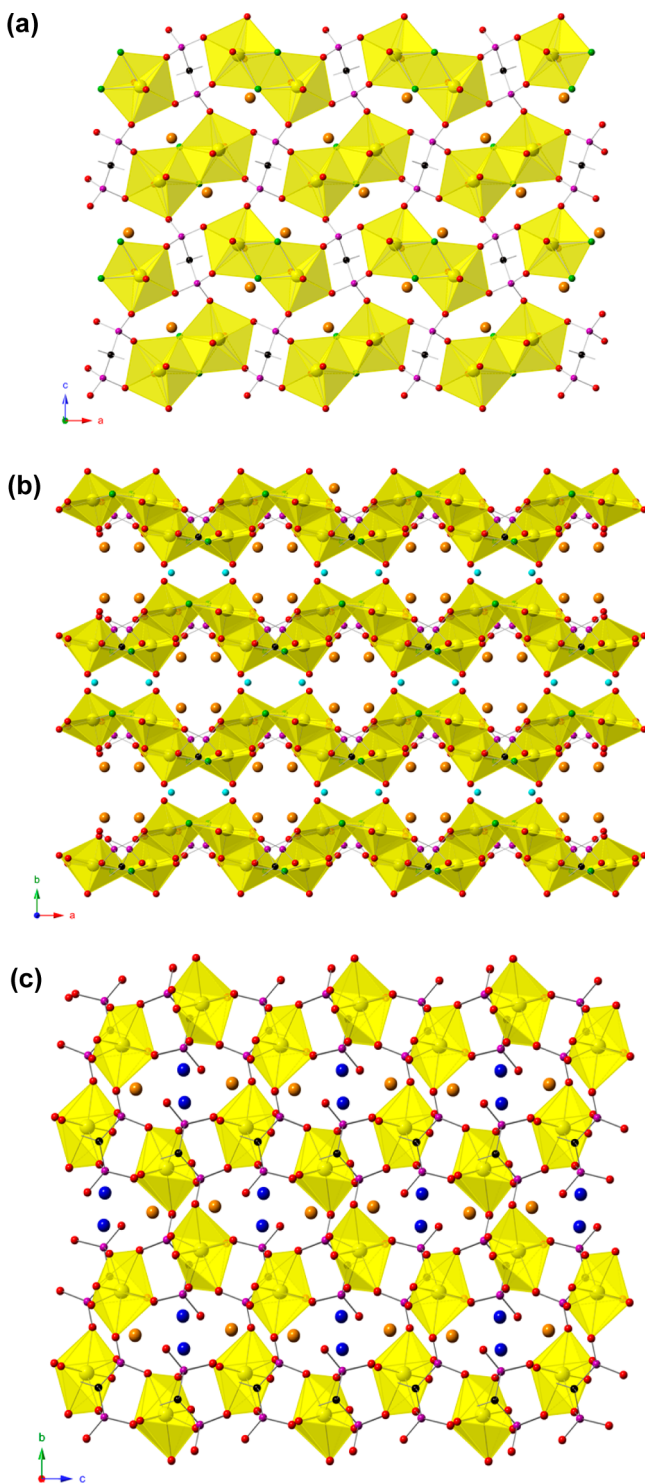


Figure 2. (a) Depiction of the sheets in $[\text{Ag}_2(\text{H}_2\text{O})_{1.5}]\{(\text{UO}_2)_2[\text{CH}_2(\text{PO}_3)_2]\text{F}_2\} \cdot (\text{H}_2\text{O})_{0.5}$ viewed along the ac plane. (b,c) Polyhedral representation of the uranyl phosphonate layers in $[\text{Ag}_2(\text{H}_2\text{O})_{1.5}]\{(\text{UO}_2)_2[\text{CH}_2(\text{PO}_3)_2]\text{F}_2\} \cdot (\text{H}_2\text{O})_{0.5}$; Ag^+ cations and a single interstitial water molecule are arranged between the layers. The structure is constructed from UO_7 pentagonal bipyramids = yellow, silver = dark orange, fluorine = green, oxygen = red, phosphorus = magenta, carbon = black, and water molecule = light blue.

sheets are stitched together by Ag^+ cations that are located in the interlayer and also charge balance the layers (see Figure 3c).

The uranyl center has a nearly linear $[\text{O}=\text{U}=\text{O}]^{2+}$ bond angle of $177.26(16)^\circ$, and the $\text{U}=\text{O}$ bond lengths are $1.782(4)$

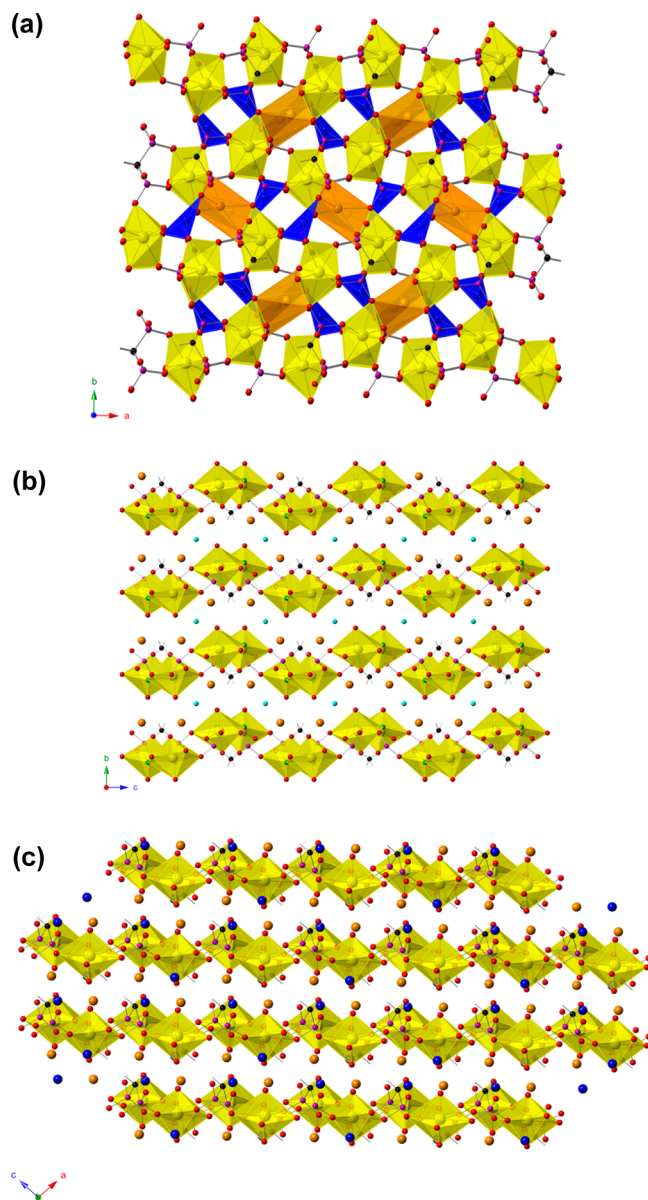


Figure 3. (a) Depiction of the sheets in $\text{Ag}_2\text{UO}_2[\text{CH}_2(\text{PO}_3)_2]$ viewed along the ab plane. (b,c) Polyhedral representation of the uranyl phosphonate layers in $\text{Ag}_2\text{UO}_2[\text{CH}_2(\text{PO}_3)_2]$ cross-linked by $\text{Ag}(1)$ and $\text{Ag}(2)$ cations; Ag^+ cations are arranged between the layers and stitch the chains together. The structure is constructed from UO_7 pentagonal bipyramids = yellow, silver (1) = dark orange, silver (2) = blue, oxygen = red, phosphorus = magenta, and carbon = black.

and $1.787(4)$ Å. The additional five oxygens are from three phosphonate groups in the pentagonal plane; two PO_3 moieties chelate the uranyl center, and one bridges. They are coordinated to the uranyl center by bond distances ranging from $2.299(3)$ to $2.506(3)$ Å. The calculated bond-valence sum for the uranium center is 5.99, which agrees with the formal oxidation state of U^{VI} .^{58,59} $\text{Ag}(1)$ is coordinated to a uranyl oxo atom through the apical position and the basal plane to four phosphonate oxygen atoms to form a square pyramidal geometry. $\text{Ag}(2)$ is coordinated to the opposite uranyl oxo atom and two phosphonate oxygen atoms to form a distorted trigonal-planar geometry. $\text{Ag}(1)$ and $\text{Ag}(2)$ form a dimer by corner sharing through $\text{P}(2)-\text{O}(5)$. The $\text{Ag}-\text{O}$ bond distances range from $2.278(4)$ to $2.581(4)$ Å and $2.191(4)$ to $2.445(4)$ Å

for Ag(1) and Ag(2), respectively. The average distance between Ag(1) and Ag(2) is 3.246(10) Å. Selected bond distances are compiled in Table 4.

UV-vis-NIR and Fluorescence Spectroscopy. The solid-state photoluminescence spectra and absorbance of all the compounds were collected at room temperature from single crystals. The absorbance spectra for all three compounds are shown in the Supporting Information, Figure S6. They reveal the characteristic equatorial U–O charge transfer bands of uranyl centered at 367, 338, and 376 nm for Ag-1, Ag-2, and Ag-3, respectively. The axial U=O charge transfer bands are observed at 432, 433, and 439 nm with characteristic vibronic fine-structure for Ag-1, Ag-2, and Ag-3, respectively.

Most uranyl containing compounds emit green light centered near 520 nm with strong vibronic coupling, yielding a well-resolved five-peak pattern at room temperature. The luminescent properties of these compounds were studied, and the spectra are illustrated in Figure 4. They all exhibit a

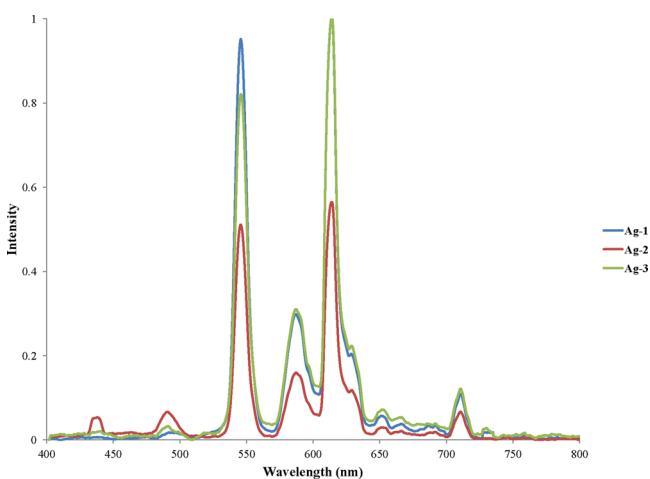


Figure 4. Solid state emission spectra of Ag-1, Ag-2, and Ag-3.

characteristic emission from UO_2^{2+} , which usually consists of several emission peaks. Six peaks are observed in the spectra for all the complexes: 491, 543, 584, 611, 650, and 708 nm for Ag-1; 488, 543, 584, 612, 650, and 708 nm for Ag-2; and 487, 544, 584, 611, 649, and 708 nm for Ag-3. These emission peaks correspond to the electronic and vibronic transitions of $S_{11}-S_{00}$ and $S_{10}-S_{0v}$ ($v = 0-4$), which are related to the symmetric and antisymmetric vibrational modes of the uranyl cation. Comparing these new silver uranyl diphosphonates with previously synthesized complexes, $\text{Ba}_3\{(\text{UO}_2)_4[\text{CH}_2(\text{PO}_3)_2]_2\text{F}_6\} \cdot 6\text{H}_2\text{O}$ (Ba-2)⁵⁷ and $[\text{C}_{10}\text{H}_{10}\text{N}_2]\{(\text{UO}_2)_2[\text{CH}_2(\text{PO}_3\text{H})_2] \cdot (\text{H}_2\text{O})\}$ (Ubp2),³⁵ these new complexes are red-shifted as compared with the previously investigated compounds, and they have a lower intensity. In Figure S7 in the Supporting Information, it is shown that there is a red shift of 87 nm for Ba-2 and 93 nm for Ubp2 when compared to Ag-2 for the most intense signal. The spectral shift may originate from the influence of the coordination of the equatorial diphosphonate ligand but also the silver cations.

Raman Spectroscopy. The strong axial U=O bonding in the majority of uranyl complexes is remarkably robust and remains reasonably unperturbed by modification of the labile equatorial ligands.⁶⁰ However, the sensitivity of the ν_1 Raman mode to the number of equatorial ligands in the uranyl(VI) complexes is well-known,⁶¹ and one generally observes a

decrease in ν_1 with successive addition of ligands to the system.⁶²⁻⁶⁴ The Raman spectra of Ag-1–Ag-3 are shown in Figure 5. Raman spectroscopy is very useful in measuring the

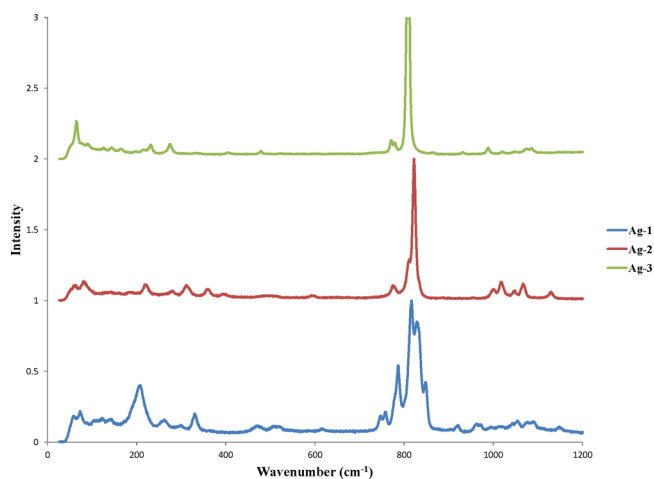


Figure 5. Raman spectra of Ag-1, Ag-2, and Ag-3.

IR-inactive UO_2^{2+} symmetric stretching frequency, resulting in sharp intense peaks. Two ν_1 frequencies are observed for Ag-1 at 816 and 829 cm^{-1} . This splitting may be a result from one of many solid-state effects that can occur in a crystalline solid. The most intense peaks at 816 and 829, 822, and 802 cm^{-1} are indicative of the ν_1 UO_2^{2+} symmetric stretch for Ag-1, Ag-2, and Ag-3, respectively. The symmetric and asymmetric stretching modes of U=O are also observed from about 750 to 920 cm^{-1} . The bands located at about 1073 cm^{-1} and in low wavenumber regions at 1001, 1017, and 1016 cm^{-1} correspond to asymmetric and symmetric P–O coordinating stretches. At regions of about 1140 cm^{-1} , these bands correspond to CH_2 stretching modes. In regions from 250 to 280 cm^{-1} , these peaks are indicative of Ag–O stretches. These values are consistent with previous studies reported by Michalska et al. where DFT calculations were done to predict vibrational frequencies in silver-containing compounds.⁶⁵ However, also in these regions of 250–280 cm^{-1} , these bands may be attributable to phonon modes of the crystal and uranyl equatorial frequencies. In Ag-1, at around 920 cm^{-1} , this band is indicative of a $\nu_{\text{sym}}(\text{P}-\text{OH})$ mode, which is complemented experimentally by the protonated P–O oxygen in the complex.

In the complexes Ag-1 to Ag-3, it is exhibited that there is a ν_1 UO_2^{2+} shift of 829 (816), 822, and 807 cm^{-1} for Ag-1, Ag-2, and Ag-3, respectively. This shift corresponds to the lengthening and weakening of the U=O bonds (1.773, 1.784, and 1.785 Å) for Ag-1, Ag-2, and Ag-3, respectively, which has been studied extensively by Clark et al. and others in uranyl-containing compounds.^{62-64,66} In Ag-2 and Ag-3, the interaction of the Ag⁺ ions with the uranyl oxygens affects the U=O bond lengthening and thus affects the Raman data: this has been reported previously.^{62,63,66} In Ag-2, there is a U=O...Ag(1) interaction with distances of 2.574 and 2.589 Å, and this corresponds to a ν_1 shift of 822 cm^{-1} . In Ag-3, U=O...Ag(1) is 2.581 Å and U=O...Ag(2) is 2.445 Å, with a Raman shift of 807 cm^{-1} . These values correspond to the lengthening of the U=O bonds and subsequent low wavenumber Raman shift seen from Ag-1 to Ag-3.

Electronic Structure. In order to obtain more insight into the nature of bonding and electronic characteristics of the

layered silver uranyl diphosphonates, electronic structure calculations were performed on the **Ag-1** and **Ag-3** compounds. The calculations on **Ag-2** could not be completed because of difficulties associated with the presence of molecular H₂O in the interlayer region, the position of which between the U–P sheets could not be clearly determined. However, based on the local geometry and coordination of the U and Ag centers, we expect many features of the electronic structure to be similar for all three compounds.

The calculations were started using the experimentally determined atomic structure, as listed in Table 1, and after allowing for the relaxation of the unit cell size and atomic positions, the structural parameters did not change appreciably. The unit cell parameters *a*, *b*, and *c* of **Ag-1** and **Ag-3** increased by 2.00, 3.10, and 0.74% and 2.00, 1.03, and 2.33%, respectively. This is expected as a consequence of the underestimation of binding energies by GGA. The nonuniform increase in the unit cell parameters can be attributed to the layered structure of the compounds. For example, in the case of **Ag-1** the largest change (3.10%) is observed along the *b* axis, which is perpendicular to the uranyl-phosphonate layers, as shown in Figure 1b. Since the interactions between the layers are weaker (possibly of van der Waals type), the GGA effect becomes more significant, resulting in a theoretical structure that is slightly elongated in the direction perpendicular to the layers.⁶⁷ Similar reasoning explains the 2.33% increase in the *c* parameter of **Ag-3** (see Figure 3c). The internal ionic relaxations result in an increase in the U–O and Ag–O bond lengths by an average of 1.9%.

The total densities of states (DOS) calculated for **Ag-1** and **Ag-3**, between –10 and +10 eV are shown in Figure 6a and b.

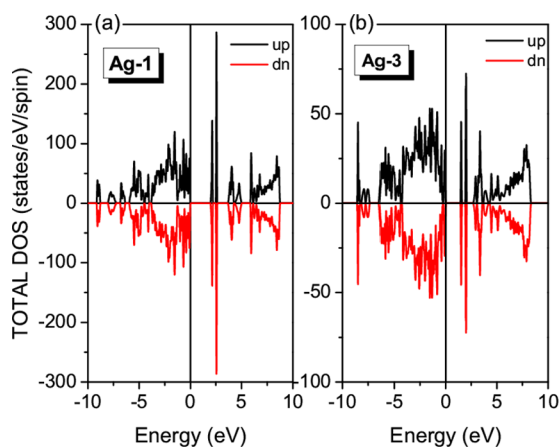


Figure 6. Total DOS of (a) **Ag-1** and (b) **Ag-3**. The major features and the overall structures of the DOSs are very similar for **Ag-1** and **Ag-3**.

The major features and the structure of the two DOS plots are very similar, consistent with the analogous structural building units of **Ag-1** and **Ag-3**. Both band structures exhibit a forbidden gap (1.98 eV for **Ag-1**; 1.45 eV for **Ag-3**), indicating that both compounds are wide bandgap semiconductors. For both, the valence bands (VB) are broad, spanning from ca. –7 eV to the Fermi level (E_F). Both VBs exhibit a narrow pseudogap in their structure at around –4 eV, which divides the VB into two parts. The main features of the conduction bands (CB) are the two large, narrow peaks located between 1.5 and 2.5 eV above E_F . At higher energies, the conduction states

exhibit hybridization and mixing and become less localized. Figure 6 shows that the DOSs associated with the majority and minority spins are identical, indicating that there is no magnetization.

In order to describe the various orbital contributions to the band structure, we analyzed the partial DOS (PDOS) associated with the O *p*, U *f*, Ag *d*, and P *p* orbitals. This is shown in Figures 7 and 8 for **Ag-1** and **Ag-3**, respectively.

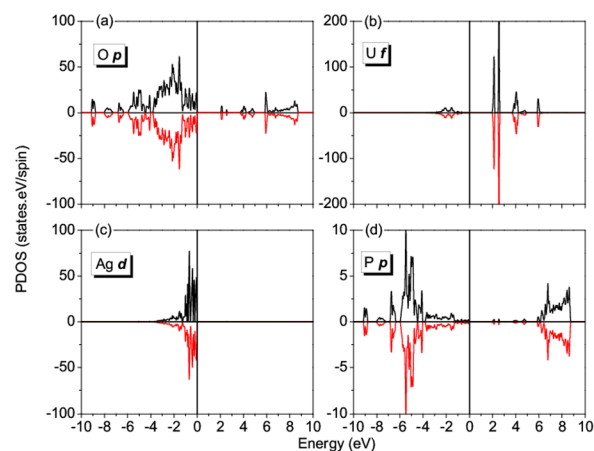


Figure 7. Partial DOS associated with the (a) O 2*p*, (b) U 5*f*, (c) Ag 4*d*, and (d) P 3*p* states in **Ag-1**.

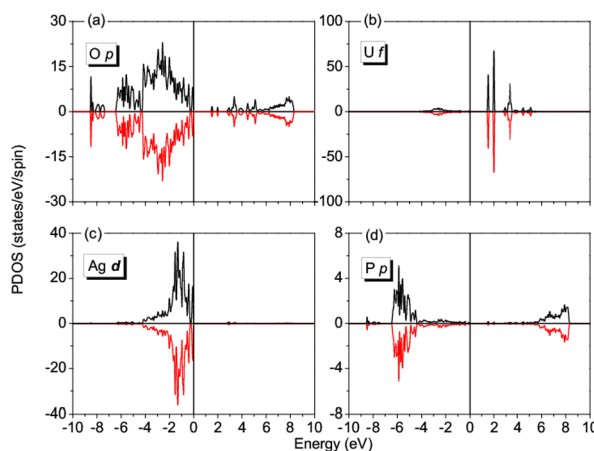


Figure 8. Partial DOS associated with the (a) O 2*p*, (b) U 5*f*, (c) Ag 4*d*, and (d) P 3*p* states in **Ag-3**.

Again, as in the case of the total DOS, the PDOSs of the two structures are very similar, the major features being almost identical. The Ag 4*d* and P 3*p* orbitals hybridize strongly with the O 2*p* orbitals. As shown in the a, c, and d panels of Figures 7 and 8, in the lower energy region of the VB (below the pseudogap), the O 2*p* orbitals mix with the P 3*p* orbitals, while in the higher energy range (above the pseudogap) the O 2*p* orbitals hybridize with the Ag 4*d* states. These P–O and Ag–O bonds are responsible for holding the uranyl pentagonal-bipyramids together, forming the layered structure. In both compounds, the Ag ions are in the Ag⁺ oxidation state, with completely filled 4*d* orbitals (Figures 7c and 8c). The narrow peaks in the CB located between 1.5 and 2.5 eV above E_F can be identified in Figures 7b and 8b as the unoccupied 5*f* states of the U ion. These states are completely empty, indicating that the uranium ions are U⁶⁺ in both compounds.

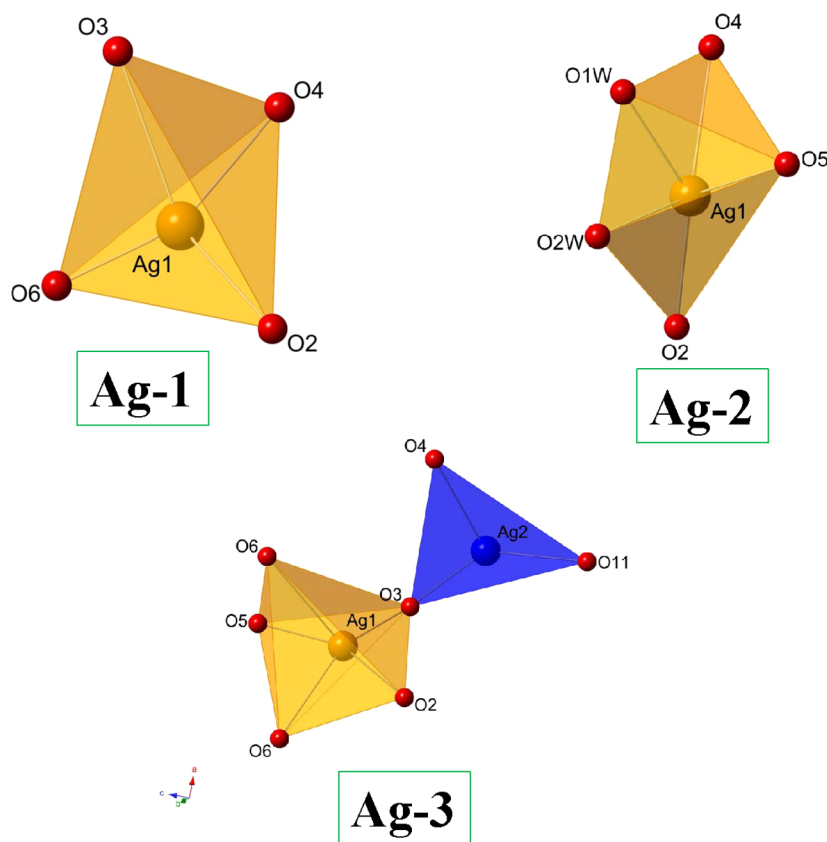


Figure 9. Polyhedral representation of the coordination geometry around the silver centers in **Ag-1**, **Ag-2**, and **Ag-3**.

■ COMMENTS ON THE COORDINATION ENVIRONMENTS AND STRUCTURES FORMED OF URANYL DISPHONATES

These compounds are all based on the methylenedisphosphate ligand (C1P2), uranyl cation, and silver(I) cations that reside in the interlayer space. Significant structural correlations are observed, which are compiled in Table 5. The silver cations in these compounds play an interesting role of stitching the anionic layers together. This is quite common in uranyl compounds.⁶⁸ The silver cations are not only playing a space-filling role, but they are directly involved in structure formation, as they are mediating the formation of the compounds by the influence of their charges.

Both **Ag-1** and **Ag-3** possess the same trimeric cluster formed by one UO_7 pentagonal bipyramid and two PO_3C tetrahedra as their structural building unit (SBU) (Table 5). The layers in both compounds stack in the AA sequence and are parallel to the *bc* and *ac* planes, respectively. In **Ag-2**, the trimeric cluster is similar to **Ag-1** and **Ag-3**, with the difference being the edge-sharing F ions bonded to the dimers of UO_5F_2 pentagons, which are bonded to two PO_3C moieties (Table 5) and then stacked in the AA sequence. In **Ag-1** and **Ag-3**, every UO_7 pentagonal bipyramid is connected by three C1P2 moieties, and every C1P2 group is bonded to three UO_7 pentagonal bipyramids. With this, every SBU is further linked to four SBUs, resulting in a layered architecture. This type of bonding has been reported by Zhang et al. where the compounds were based on the 1-hydroxyethylidenediphosphate ligand.⁶⁹ In **Ag-2**, every C1P2 group is connected to four UO_5F_2 edge-shared dimers, and every dimer is bonded to four C1P2 ligands.

Thus, every SBU is further linked to six SBUs, resulting in a layered architecture.

Ag-1 and **Ag-3** have similar structural units and close framework formulas but represent different structures. In **Ag-1**, there is a protonated P–OH group which renders that phosphonate oxygen atom from further bonding. This protonation is evidenced by the longer P–O bond distance that is common for partially protonated phosphonate groups.⁷⁰ While in **Ag-3**, there is a phosphonate oxygen oriented in the interlayer space that coordinates solely to Ag^+ centers. This result is similar to $\text{Ba}[\text{UO}_2[\text{CH}_2(\text{PO}_3)_2]\cdot 1.4\text{H}_2\text{O}]$, where the phosphonate oxygen binds either to uranium or barium/silver and less often to both with $\mu_2\text{-O}$ atoms.⁵⁷ These results differ from previously reported observations for which the PO_3 groups of diphosphonate always bond to the harder uranium center, according to the Hard/Soft Acid/Base Theory,⁷¹ and may also coordinate to a second metal center with $\mu_2\text{-O}$ atoms.

There are distinct topologies in these three compounds. Although all have two-dimensional anionic sheets with layered architectures, the structures are different. In **Ag-1**, there is a single UO_7 center bonded by a single C1P2 ligand. A site of protonation on the PO_3C group renders that oxygen from further bonding and orients in the interlayer space. The single Ag^+ center is four-coordinated and only bonds to phosphonate oxygens, two from each PO_3C group. In **Ag-2**, the uranium center forms dimers edge-shared through F atoms and is chelated and bridged through C1P2 moieties to four more UO_5F_2 dimers. There is a single Ag^+ center as in **Ag-1**, but it is five coordinated through uranyl oxo groups, a phosphonate oxygen, and two terminal aqua molecules. In **Ag-3**, the structure is similar to **Ag-1**, with the exception of a phosphonate oxygen binding solely to Ag^+ centers (depicted

by highlighted oxygen in Table 5) and the presence of two Ag^+ centers. The Ag^+ center forms a dimer through $\mu_2\text{-O}$ of a phosphonate oxygen atom. **Ag(1)** is five coordinate and bonds to a uranyl oxo atom and phosphonate oxygen atoms. **Ag(2)** is three coordinate, bonding to the a uranyl oxo atom and two phosphonate oxygen atoms. A polyhedral representation of the coordination geometry around the silver centers is illustrated in Figure 9.

In addition to the aforementioned comparisons of the structures, we note that the pH of the reactions can also affect the type of structures that form. In **Ag-1**, where the solvent used was water, an anionic sheet of $\text{UO}_2[\text{CH}_2(\text{PO}_3)(\text{PO}_3\text{H})]^-$ was obtained and is similar to previous results where a protonation site is observed in a more acidic medium. This has been observed with templated uranyl diphosphonates,³⁵ as well as earlier synthesized uranium diphosphonates: $\text{UO}_2[\text{CH}_2(\text{PO}_3\text{H}_2)](\text{H}_2\text{O})$.¹² At a reduced pH, there is an effect of having protonation sites that are incapable of further bonding and, thus, are terminal sites. In **Ag-2**, the addition of HF increases the degree of crystallinity, but the F also serves as a ligand and is an essential constituent of the **Ag-2** structure. This occurs when F atoms are incorporated into the structures of uranyl diphosphonates and carboxyphosphonates.^{28,57} In **Ag-3**, the addition of LiOH causes an increase in pH, resulting in a complete deprotonation of PO_3C groups, which allows for additional bonding. This is consistent with previous work on uranyl diphosphonates in which the addition of $\text{Ba}(\text{OH})_2 \cdot 6\text{H}_2\text{O}$ to methylenediphosphonic acid led to the isolation of $\text{Ba}[\text{UO}_2[\text{CH}_2(\text{PO}_3)_2] \cdot 1.4\text{H}_2\text{O}]$, in which all the phosphonate oxygens are completely deprotonated and bonds to uranium and barium centers.⁵⁷ In essence, low-pH syntheses yield structures in which some phosphonates are protonated and coordinates preferentially, but not exclusively, to the uranium center. For high-pH syntheses, protonation is completely eliminated and phosphonates are bonded to the uranium center and/or a second metal center.

CONCLUSIONS

The synthesis of a series of uranyl silver diphosphonates has allowed the elucidation of the influence of monovalent cations on the topologies of uranyl diphosphonates. Significantly, these structures are closely related: **Ag-1** and **Ag-3** possess the same SBU, but different structures, in which **Ag-1** is a layered structure where a site of protonation occurs around a PO_3C group, and Ag^+ ions are located between the layers and bonds only to phosphonate oxygens. In contrast, in **Ag-3**, there is complete elimination of protonated sites, and a phosphonate oxygen bonds solely to Ag^+ centers. The Ag^+ centers form dimers that are corner-shared through a $\mu_2\text{-O}$ phosphonate oxygen, and it is located between the layers. In **Ag-2**, the SBU is a trimeric cluster but differs from the other two compounds where dimers of UO_5F_2 are formed and edge-shared through F atoms. The pH plays an important role in these syntheses as demonstrated with **Ag-1** and **Ag-3**, where protonation is either completely or partially eliminated and allows for additional bonding of metal centers. The structural differences are attributed to the polymerization of UO_2^{2+} sites in **Ag-2** to form $(\text{UO}_2)_2\text{O}_6\text{F}_2$ dimers, the ligation of F anions around the uranium metal centers in **Ag-2**, and the Ag^+ -ligand coordination observed in **Ag-3** with Ag^+ centers forming dimers through $\mu_2\text{-O}$ phosphonate oxygen.

Electronic structure calculations provide a complement to the experiments showing the hybridization of the $\text{Ag } 4d$ and P

$3p$ orbitals with the $\text{O } 2p$ orbitals. With this, the P-O and Ag-O bonds are responsible for holding the uranyl pentagonal bipyramids together. This is demonstrated experimentally, as the silver center influences the structures formed, along with further ligation of the phosphonate groups around the uranium center.

ASSOCIATED CONTENT

Supporting Information

X-ray crystallographic files for **Ag-1**, **Ag-2**, and **Ag-3** in CIF format (CCDC 946887–946889); PXRD pattern; bond-valence sum for silver atoms; fluorescence spectrum; absorbance spectrum; and EDX pattern for **Ag-2** are included. This material is free of charge via the Internet at <http://pubs.acs.org>.

AUTHOR INFORMATION

Corresponding Author

*Address: 2534 C.C. Little Building, University of Michigan, Ann Arbor, MI 48109-1005. Phone: 734-615-2048. E-mail: nelsa@umich.edu.

Notes

The authors declare no competing financial interest.

ACKNOWLEDGMENTS

This work was supported by the Center on Materials Science of Actinides, an Energy Frontier Research Center funded by the U.S. Department of Energy, Office of Science, Office of Basic Energy Sciences under Award Number DE-SC0001089. The computational analysis was performed at the National Energy Research Scientific Computing Center, which is supported by the Office of Science of the U.S. Department of Energy under Contract No. DE-AC02-05CH11231 (Z.R.). We are grateful for support provided by the Chemical Sciences, Geosciences, and Biosciences Division, Office of Basic Energy Sciences, Office of Science, Heavy Elements Chemistry Program, U.S. Department of Energy, under Grant DE-FG02-09ER16026 (to T.E.A.-S.). We further acknowledge Dr. Udo Becker for his review of the computational results.

REFERENCES

- (1) Yin, P.; Zheng, L. M.; Gao, S.; Xin, X. Q. *Chem. Commun.* **2001**, 2346.
- (2) Shi, X.; Zhu, G. S.; Qiu, S. L.; Huang, K. L.; Yu, J. H.; Xu, R. R. *Angew. Chem., Int. Ed.* **2004**, *43*, 6482.
- (3) Bujoli, B.; Lane, S. M.; Nonglaton, G.; Pipelier, M.; Léger, J.; Talham, D. R.; Tellier, C. *Chem.—Eur. J.* **2005**, *11*, 1980.
- (4) Mao, J. G. *Coord. Chem. Rev.* **2007**, *251*, 1493.
- (5) Plabst, M.; McCusker, L. B.; Bein, T. *J. Am. Chem. Soc.* **2009**, *131*, 18112.
- (6) (a) Adelani, P. O.; Albrecht-Schmitt, T. E. *Angew. Chem., Int. Ed.* **2010**, *49*, 8909–8911. (b) Adelani, P. O.; Albrecht-Schmitt, T. E. *Inorg. Chem.* **2011**, *50*, 12184–12191.
- (7) (a) Clearfield, A. *Curr. Opin. Solid State Mater. Sci.* **1996**, *1*, 268. (b) Clearfield, A. *Prog. Inorg. Chem.* **1998**, *47*, 371. (c) Clearfield, A.; Demadis, K. *Metal Phosphonate Chemistry: From Synthesis to Applications*; The Royal Society of Chemistry: Cambridge, U.K., 2012.
- (8) Nash, K. L. *J. Alloys Compd.* **1994**, *213–214*, 300–304.
- (9) Nash, K. L. *J. Alloys Compd.* **1997**, *249*, 33–40.
- (10) Jensen, M. P.; Beitz, J. V.; Rogers, R. D.; Nash, K. L. *J. Chem. Soc., Dalton Trans.* **2000**, *18*, 3058–3064.
- (11) Bao, S.-S.; Zheng, L. M.; Liu, Y. J.; Xu, W.; Feng, S. *Inorg. Chem.* **2003**, *42*, 5037–5039.

- (12) Nelson, A.-G. D.; Bray, T. H.; Zhan, W.; Haire, R. G.; Saylor, T. S.; Albrecht-Schmitt, T. E. *Inorg. Chem.* **2008**, *47*, 4945–4951.
- (13) Nelson, A.-G. D.; Bray, T. H.; Albrecht-Schmitt, T. E. *Angew. Chem., Int. Ed.* **2008**, *47*, 6252–6254.
- (14) Nelson, A.-G. D.; Bray, T. H.; Stanley, F. A.; Albrecht-Schmitt, T. E. *Inorg. Chem.* **2009**, *48*, 4530–4535.
- (15) Diwu, J.; Nelson, A.-G.; Albrecht-Schmitt, T. E. *Comm. Inorg. Chem.* **2009**, *31*, 46.
- (16) Diwu, J.; Nelson, A.-G.; Wang, S.; Campana, C.; Albrecht-Schmitt, T. E. *Inorg. Chem.* **2010**, *49*, 3337.
- (17) (a) Libson, K.; Deutsch, E.; Barnett, B. L. *J. Am. Chem. Soc.* **1980**, *102*, 2476. (b) Harvey, H. G.; Teat, S. J.; Tang, C. C.; Cranswick, L. M.; Atfield, M. P. *Inorg. Chem.* **2003**, *42*, 2428. (c) Dumas, E.; Sassoie, C.; Smith, K. D.; Sevov, S. C. *Inorg. Chem.* **2002**, *41*, 4029.
- (18) (a) Soghomonian, V.; Chen, Q.; Haushalter, R. C.; Zubieta, J. *Angew. Chem., Int. Ed. Engl.* **1995**, *34*, 223. (b) Finn, R. C.; Lam, R.; Greedan, J. E.; Zubieta, J. *Inorg. Chem.* **2001**, *40*, 3745. (c) Finn, R. C.; Rarig, R. S., Jr.; Zubieta, J. *Inorg. Chem.* **2002**, *41*, 2109.
- (19) (a) Serre, C.; Férey, G. *Inorg. Chem.* **1999**, *38*, 5370. (b) Riou, D.; Serre, C.; Férey, G. *Int. J. Inorg. Mater. Chem.* **2000**, *2*, 551. (c) Barthelet, K.; Riou, D.; Férey, G. *Solid State Sci.* **2002**, *4*, 841.
- (20) Lohse, D. L.; Sevov, S. C. *Angew. Chem., Int. Ed. Engl.* **1997**, *36*, 1619.
- (21) Knope, K. E.; Cahill, C. L. *Inorg. Chem.* **2008**, *47*, 7660–7672.
- (22) Knope, K. E.; Cahill, C. L. *Inorg. Chem.* **2009**, *48*, 6845–6851.
- (23) Alsobrook, A. N.; Zhan, W.; Albrecht-Schmitt, T. E. *Inorg. Chem.* **2008**, *47*, 5177–5183.
- (24) Alsobrook, A. N.; Hauser, B. G.; Hupp, J. T.; Alekseev, E. V.; Depmeier, W.; Albrecht-Schmitt, T. E. *Cryst. Growth Des.* **2011**, *11*, 1385.
- (25) Alsobrook, A. N.; Hauser, B. G.; Hupp, J. T.; Alekseev, E. V.; Depmeier, W.; Albrecht-Schmitt, T. E. *Chem. Commun.* **2010**, *46*, 9167.
- (26) Alsobrook, A. N.; Alekseev, E. V.; Depmeier, W.; Albrecht-Schmitt, T. E. *J. Solid State Chem.* **2011**, *184*, 1195.
- (27) Knope, K. E.; Cahill, C. L. *Inorg. Chem.* **2010**, *49*, 1177.
- (28) Adelani, P. O.; Albrecht-Schmitt, T. E. *Cryst. Growth Des.* **2011**, *11*, 4676–4683.
- (29) Zhu, Y. Y.; Sun, Z. G.; Zhao, Y.; Zhang, J.; Lu, X.; Zhang, N.; Liu, L.; Tong, F. *New J. Chem.* **2009**, *33*, 119.
- (30) Zhu, Y. Y.; Sun, Z. G.; Chen, H.; Zhang, J.; Zhao, Y.; Zhang, N.; Liu, L.; Lu, X.; Wang, W. N.; Tong, F.; Zhang, L. C. *Cryst. Growth Des.* **2009**, *7*, 3228.
- (31) Liu, L.; Sun, Z. G.; Zhang, N.; Zhu, Y. Y.; Zhao, Y.; Lu, X.; Tong, F.; Wang, W. N.; Huang, C. Y. *Cryst. Growth Des.* **2010**, *10*, 406.
- (32) (a) Song, H.-H.; Zheng, L.-M.; Wang, Z.; Yan, C.-H.; Xin, X.-Q. *Inorg. Chem.* **2001**, *40*, 5024–5029. (b) Bauer, S.; Müller, H.; Bein, T.; Stock, N. *Inorg. Chem.* **2005**, *44*, 9464–9470. (c) Sharma, C. V. K.; Clearfield, A. *J. Am. Chem. Soc.* **2000**, *122*, 4394–4402. (d) Barthelet, K.; Merlier, C.; Serre, C.; Riou-Cavellec, M.; Riou, D.; Férey, G. *J. Mater. Chem.* **2002**, *12*, 1132–1137. (e) Barthelet, K.; Riou, D.; Férey, G. *Solid State Sci.* **2002**, *4*, 841–844.
- (33) Doran, M. B.; Norquist, A. J.; O'Hare, D. *Chem. Mater.* **2003**, *15*, 1449.
- (34) Adelani, P. O.; Albrecht-Schmitt, T. E. **2009**482732–2734.
- (35) Nelson, A.-G. D.; Alekseev, E. V.; Albrecht-Schmitt, T. E.; Ewing, R. C. *J. Solid State Chem.* **2013**, *198*, 270–278.
- (36) Sheldrick, G. M. *Acta Crystallogr.* **1995**, *A51*, 33.
- (37) Sheldrick, G. M. *P.C. SHELXTL*, version 6.12; Siemens Analytical X-ray Instruments, Inc: Madison, WI, 2001.
- (38) Blochl, P. E. *Phys. Rev. B* **1994**, *50*, 17953.
- (39) Kresse, G.; Joubert, D. *Phys. Rev. B* **1991**, *59*, 1758.
- (40) Hohenberg, P.; Kohn, W. *Phys. Rev. B* **1964**, *136*, B864.
- (41) Kohn, W.; Sham, L. J. *Phys. Rev.* **1965**, *140*, 1133.
- (42) Kresse, G.; Furthmüller, J. *Phys. Rev. B* **1996**, *54*, 11169.
- (43) Kresse, G.; Furthmüller, J. *Comput. Mater. Sci.* **1996**, *6*, 15.
- (44) Kresse, G.; Hafner, J. *Phys. Rev. B* **1993**, *47*, 558.
- (45) Kresse, G.; Hafner, J. *Phys. Rev. B* **1994**, *49*, 14251.
- (46) Perdew, J. P.; Burke, K.; Ernzerhof, M. *Phys. Rev. Lett.* **1996**, *77*, 3865.
- (47) Monkhorst, H. J.; Pack, J. D. *Phys. Rev. B* **1976**, *13*, 5188.
- (48) Anisimov, V. I.; Aryasetiawan, F.; Liechtenstein, A. I. *J. Phys. Cond. Mater.* **1997**, *767*.
- (49) Anisimov, V. I.; Zaanen, J.; Andersen, O. K. *Phys. Rev. B* **1991**, *44*, 943.
- (50) Liechtenstein, A. I.; Anisimov, V. I.; Zaanen, J. *Phys. Rev. B* **1995**, *52*, R5467.
- (51) Anisimov, V. I.; Gunnarsson, O. *Phys. Rev. B* **1991**, *43*, 7570.
- (52) Anisimov, V. I.; Elfimov, I. S.; Hamada, N.; Terakura, K. *Phys. Rev. B* **1996**, *54*, 4387.
- (53) Dorado, B.; Jomard, G.; Freyss, M.; Bertolus, M. *Phys. Rev. B* **2010**, *82*, 035114.
- (54) Rak, Zs.; Ewing, R. C.; Becker, U. *Phys. Rev. B* **2011**, *83*, 155123.
- (55) Rak, Zs.; Ewing, R. C.; Becker, U. *Surf. Sci.* **2013**, *608*, 180.
- (56) Jiao, C.; Sun, Z.; Zhu, Y.; Chen, K.; Zhu, J.; Li, C.; Wang, C.; Sun, S.; Tian, H.; Chu, W.; Zheng, M.; Shao, W.; Lu, Y. *Inorg. Chim. Acta* **2012**, *387*, 186–194.
- (57) Nelson, A.-G. D.; Alekseev, E. V.; Ewing, R. C.; Albrecht-Schmitt, T. E. *J. Solid State Chem.* **2012**, *192*, 153–160.
- (58) (a) Burns, P. C.; Ewing, R. C.; Hawthorne, F. C. *Can. Mineral.* **1997**, *35*, 1551. (b) Burns, P. C.; Miller, M. L.; Ewing, R. C. *Can. Mineral.* **1996**, *34*, 845. (c) Burns, P. C. *Can. Mineral.* **2005**, *43*, 1839.
- (59) Brese, N. E.; O'Keeffe, M. *Acta Crystallogr.* **1991**, *B47*, 192.
- (60) Denning, R. G. *Struct. Bonding (Berlin)* **1992**, *79*, 215.
- (61) Nguyen-Trung, C.; Begun, G. M.; Palmer, D. A. *Inorg. Chem.* **1992**, *31*, 5280.
- (62) Clark, D. L.; Conradson, S. D.; Donohoe, R. J.; Keogh, D. W.; Morris, D. E.; Palmer, P. D.; Rogers, R. D.; Tait, C. D. *Inorg. Chem.* **1999**, *38*, 1456.
- (63) Burns, C. J.; Clark, D. L.; Donohoe, R. J.; Duval, P. B.; Scott, B. L.; Tait, C. D. *Inorg. Chem.* **2000**, *39*, 5464.
- (64) Clark, D. L.; Conradson, S. D.; Donohoe, R. J.; Gordon, P. L.; Keogh, D. W.; Palmer, P. D.; Scott, B. L.; Tait, C. D. *Inorg. Chem.* **2013**, *52*, 3547.
- (65) Morzyk-Ociepa, B.; Michalska, D. *Spectrochim. Acta, Part A* **2003**, *59*, 1247–1254.
- (66) Danis, J. A.; Lin, M. R.; Scott, B. L.; Eichhorn, B. W.; Runde, W. H. *Inorg. Chem.* **2001**, *40*, 3389–3394.
- (67) Anderson, Y.; Langreth, D. C.; Lundqvist, B. I. *Phys. Rev. Lett.* **1996**, *76*, 102.
- (68) (a) Burns, P. C. *Uranium: Mineralogy, Geochemistry, and the Environment*; Burns, P. C., Finch, R., Eds.; Mineralogical Society of America: Washington, DC, 1999; Chapter 1. (b) Burns, P. C. *Mater. Res. Soc. Symp. Proc.* **2004**, *89*, 802.
- (69) Yang, W.; Wu, H. Y.; Wang, R. X.; Pan, Q. J.; Sun, Z. M.; Zhang, H. *Inorg. Chem.* **2012**, *51*, 11458–11465.
- (70) Kong, D.; Yao, J.; Clearfield, A.; Zon, J. *Cryst. Growth Des.* **2008**, *8*, 2892–2898.
- (71) Pearson, R. G. *J. Chem. Educ.* **1968**, *45*, 581.

NOTE ADDED AFTER ASAP PUBLICATION

This paper was published on the Web on February 13, 2014. An additional co-author was added to the paper, and the corrected version was reposted on February 27, 2014.